



Environmental effects on low cycle fatigue of 2024-T351 and 7075-T651 aluminum alloys

E.U. Lee ^{a,*}, A.K. Vasudevan ^b, G. Glinka ^c

^a Naval Air Warfare Center Aircraft Division, Patuxent River, MD 20670, USA

^b Office of Naval Research, 875 N. Randolph Street, Arlington, VA 22203, USA

^c University of Waterloo, 200 University Avenue West, Waterloo, Ontario, Canada N2L 3G1

ARTICLE INFO

Article history:

Received 23 September 2008

Received in revised form 18 November 2008

Accepted 21 November 2008

Available online 7 December 2008

Keywords:

Low cycle fatigue

Environmental effect

Strain amplitude

Fractographic features

ABSTRACT

The environmental effects on the low cycle fatigue (LCF) behavior of 2024-T351 and 7075-T651 aluminum alloys were studied at room temperature. The specimens were subjected to identical LCF tests at strain ratio R of -1 and frequency of 5 Hz in three environments: vacuum, air and 1% NaCl solution of pH 2. A separate group of specimens was pre-corroded in 1% NaCl solution and then LCF-tested in air. Their strain–life relations and cyclic stress–strain responses were investigated and compared. Furthermore, the fracture surface morphology was evaluated to find the association of LCF behavior and fractographic features under different environmental conditions.

Published by Elsevier Ltd.

1. Introduction

Significant influences of environment on fatigue behavior of metals have been found in many metal/environment systems. The fatigue crack growth rate can be higher in a corrosive environment than in an inert environment, such as vacuum, and it depends on the chemical and electrochemical variables in the environment. The environment-assisted fatigue cracking is attributed to single or mutual occurrence of anodic dissolution and/or hydrogen-induced cracking at the crack tip. Especially, for high strength aluminum alloys, corrosion generates hydrogen which interacts with the plastic zones of growing cracks leading to a form of localized hydrogen embrittlement [1].

The environmental effect on the high cycle fatigue (HCF) was extensively investigated in various environments [2–14]. Particularly, it was established that a testing in vacuum leads to a longer HCF life and a corrosive environment can accelerate or retard the HCF crack growth. Besides, the fractographic features of a metal, subjected to HCF, were also found to be sensitive to the environmental conditions. Flat and featureless morphology was observed after HCF in vacuum, striations after HCF in air and cleavages after HCF in 3.5% NaCl solution for various alloys [15–17]. On the one hand, the LCF lives of polycrystalline 316L stainless steel speci-

mens were reported to be longer in vacuum, compared with in air, by factors of ~ 2 or 3 at room temperature [18]. However, the environmental influence on LCF behavior has been studied mostly in vacuum, air and enriched oxygen at elevated temperatures [19,20], but little in more corrosive environments, such as NaCl solution, at ambient temperature.

LCF data can be presented graphically as strain–life and cyclic stress–strain curves, and characterized by the following Coffin–Manson [21,22] and Ramberg–Osgood [23] relationships.

$$\Delta\varepsilon/2 = (\sigma'_f/E)(2N)^b + \varepsilon'_f(2N)^c \quad (1)$$

where $\Delta\varepsilon/2$ = strain amplitude, σ'_f = fatigue strength coefficient, E = modulus of elasticity, N = strain cycles to failure, b = fatigue strength exponent, ε'_f = fatigue ductility coefficient and c = fatigue ductility exponent.

$$\varepsilon = (\sigma/E) + (\sigma/\kappa')^{1/n} \quad (2)$$

where ε = peak cyclic tensile strain, σ = stabilized peak cyclic tensile stress, E = modulus of elasticity, κ' = cyclic strength coefficient and n = cyclic strain hardening exponent.

It is desirable to find whether or how much these relationships and fractographic features are affected by environment. In this study, an effort is made to clarify the environmentally-influenced LCF behavior, especially the strain–life relation, cyclic stress–strain response and fractographic features, for two aluminum alloys, 2024-T351 and 7075-T651, at room temperature in vacuum, air and 1% NaCl solution.

* Corresponding author. Tel.: +1 301 342 8069; fax: +1 301 342 8062.

E-mail address: enu.lee@navy.mil (E.U. Lee).

2. Experimental procedure

2.1. Testing materials and specimens

Slabs of 2024-T351 and 7075-T651 aluminum alloys were chosen as the specimen materials, because they were widely used for various aircraft components exposed to service environments, some harsh. From the slabs, round rod specimens of gage section diameter 6.4 mm (0.25 in.) and length 12.7 mm (0.5 in.) were machined in the *T*-orientation. The geometry and dimension of the specimen are shown in Fig. 1. The specimen surface was highly polished longitudinally with emery cloths to a mirror finish. Their mechanical properties were

	Yield strength		UTS	
	ksi	MPa	ksi	MPa
2024-T351	47	327	68	470
7075-T651	77	530	88	610

2.2. Test environments

Vacuum of 4×10^{-8} torr, air of relative humidity of 50–60% and aqueous 1% NaCl solution of pH 2 were selected as the test environments. Vacuum was taken to characterize the pure LCF behavior, free from environmental effect. Air and 1% NaCl solution were taken to quantify the effects of mild and severe environments, respectively.

2.3. LCF tests

Two closed-loop servo-hydraulic mechanical test machines were employed for the fatigue tests. One was a 490 kN MTS machine with a vacuum system for the test in vacuum, and the other a 100 kN machine for the tests in still air and circulating aqueous 1% NaCl solution of pH 2. The vacuum system consisted of a vertical vacuum chamber of stainless steel, a mechanical pump, a molecular turbo-pump and vacuum gages. The vacuum chamber had sufficient space, $86 \times 43 \times 36$ cm ($34 \times 17 \times 14$ in.), for a pair of hydraulic grips with a specimen under static or cyclic loading, and was able to hold a vacuum of 4×10^{-8} torr. The LCF tests were conducted under constant amplitude cyclic straining of $R = -1$ and frequency 5 Hz at ambient temperature in respective environments, following ASTM Standard E 606-92 (standard practice for strain-controlled fatigue testing). In these tests, the complete fracture-separation of the specimen under LCF straining was defined as the LCF failure.

A group of 7075-T651 aluminum alloy specimens was pre-corroded in the 1% NaCl solution of pH 2 for the period, equal to the time of LCF test at a given strain amplitude in the 1% NaCl solution. Subsequently, those specimens were LCF-tested in air.

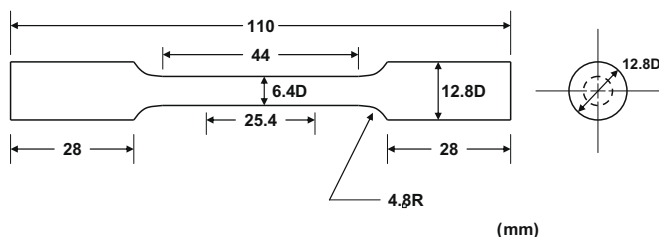


Fig. 1. LCF test specimen.

2.4. Fractography

After the LCF failure of the 7075-T651 aluminum alloy specimen, its fracture surface morphology was examined with a scanning electron microscope, JEOL JSM-6460LV, operated at an accelerating voltage of 20 kV. The examination was conducted at different magnifications to identify the unique fractographic features, representing the immediate vicinity of crack initiation site and the outside area, for each environment. Subsequently, the fractographic features for the three environments were compared.

3. Result and discussion

3.1. LCF life

The curves of strain amplitude vs. strain-reversal (or two times the number of strain cycles to fracture) are shown in Fig. 2 for the LCF tests of 2024-T351 and 7075-T651 aluminum alloys in the three environments: vacuum, air and 1% NaCl solution. The curves for the tests in vacuum and air are nearly overlapping, though the air curve is located slightly below the vacuum curve at lower strain amplitudes. The curve for the test in 1% NaCl solution is located far below the two curves. Their difference is greater at lower strain amplitudes. This observation evidences that the LCF life is longest in vacuum, slightly shorter in air and shortest in 1% NaCl solution for a given strain amplitude. From those curves, the equations of strain–life in the three environments are found as follows.

Environment	LCF fracture	
	2024-T351	7075-T651
Vacuum	$\Delta\epsilon/2 = (2.541 \times 10^{-2})(2N)^{-0.154}$	$(2.547 \times 10^{-2})(2N)^{-0.142}$
Air	$\Delta\epsilon/2 = (4.786 \times 10^{-2})(2N)^{-0.236}$	$(2.965 \times 10^{-2})(2N)^{-0.169}$
1% NaCl	$\Delta\epsilon/2 = (1.247 \times 10^{-1})(2N)^{-0.387}$	$(1.260 \times 10^{-1})(2N)^{-0.402}$

The intercept (or fatigue ductility coefficient) and slope (or fatigue ductility exponent) of the strain–life curve are least in vacuum and greatest in 1% NaCl solution.

The strain–life curve for the pre-corroded and air-tested specimens of 7075-T651 aluminum alloy is also included in Fig. 2. The curve is located slightly below the vacuum curve, nearly overlapping the air curve, and far above the 1% NaCl solution curve. This observation evidences the little influence of the initial pre-corrosion on the subsequent LCF life in air. Furthermore, it can be deduced that the reduction of LCF life in 1% NaCl solution is mainly attributed to the interaction of the NaCl solution and the crack surface, such as access of 1% NaCl solution to the crack tip, adsorption, surface dissociation and hydrogen production, hydrogen entry at the crack tip and embrittling reaction [8].

Throughout this study, only one straining frequency, 5 Hz, was used for all LCF tests to avoid the frequency effect on LCF behavior, especially the crack growth. Although a change in frequency in the inert environment has no major influence on fatigue crack growth, lowering the frequency (i.e., increasing the time for environmental interactions with crack surface per stress- or strain-cycle) in a corrosive environment, such as NaCl solution, causes an appreciable increase in the crack growth rate [24].

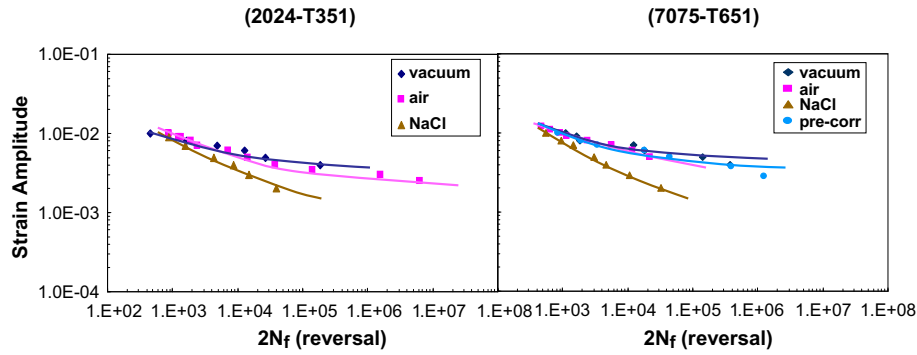


Fig. 2. Strain–life curves for 2024-T351 and 7075-T651 aluminum alloys, LCF-tested in vacuum, air and 1% NaCl solution.

3.2. Comparison of LCF lives of 2024-T351 and 7075-T651 aluminum alloys

Though 2024-T351 and 7075-T651 aluminum alloys have different chemical compositions and mechanical properties (YS and UTS), their strain–life curves nearly overlap, indicating their similar LCF lives or resistances, in each of the three environments, Fig. 3.

3.3. Cyclic stress–strain curves

Under controlled cyclic straining, the specimen was observed to be work-softened initially and stabilized eventually, creating a virtually constant peak and minimum stress condition for the remainder of the straining in the three environments. The stabilized peak cyclic tensile stress, as measured at the half-life stage of the individual LCF test, is plotted against the applied peak tensile strain in Fig. 4 for the 2024-T351 and 7075-T651 aluminum alloys. From those curves, it is clear that

- The cyclic stress–strain curves for the three environments overlap each other, indicating the cyclic stress–strain response independent of environment for a given alloy.
- The cyclic stress–strain curve of 7075-T651 aluminum alloy is located above that of 2024-T351 aluminum alloy, indicating that the peak tensile stress is greater at a given peak tensile strain for the 7075-T651 aluminum alloy than for the 2024-T351 aluminum alloy. Evidently, the cyclic stress–strain response is unique to a given alloy.

Furthermore, these curves can be characterized by the aforementioned Ramberg–Osgood relationship, Eq. (2). The values of E , κ' and n of the equation for the two alloys are

	E (GPa)	κ'	n
2024-T351	72.4	957	0.166
7075-T651	71.0	5714	0.494

Apparently, the Ramberg–Osgood relationship is independent of environment but unique to the alloy.

3.4. Variation of stress amplitude with time

From Eq. (2), the stress amplitude, $\Delta\sigma/2$, corresponding to an applied strain amplitude, $\Delta\varepsilon/2$, was found. Its variation with time of LCF straining, converted from the applied strain-cycle, is plotted in Fig. 5. In all three environments, vacuum, air and 1% NaCl solution, the stress amplitude decreased with increasing time of LCF straining, indicating the load carrying capacity decreasing with time due to crack growth for the both alloys. The reduction rate of stress amplitude, or the slope of the curve, is much greater in 1% NaCl solution than in vacuum and air, evidencing the greater environmentally assisted LCF crack growth in 1% NaCl solution.

3.5. Fractographic features of 7075-T651 aluminum alloy

The fracture surface of the 7075-T651 aluminum alloy specimen, LCF-tested in vacuum, is flat and featureless in the immediate

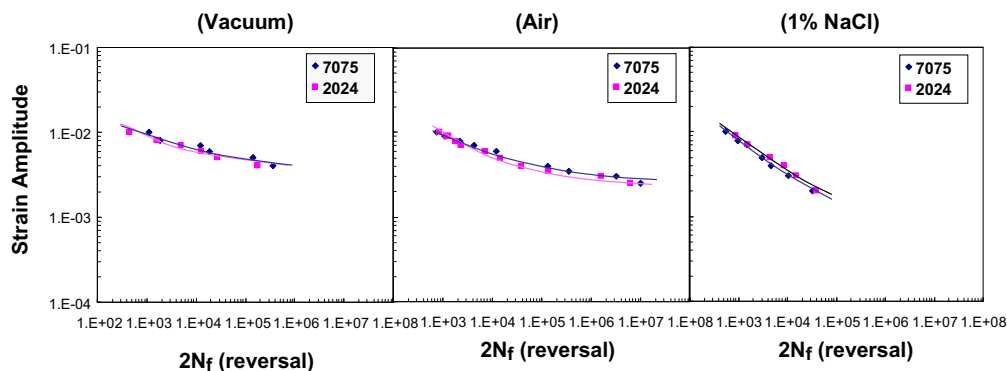


Fig. 3. Comparison of LCF lives of 2024-T351 and 7075-T651 aluminum alloys in vacuum, air and 1% NaCl solution.

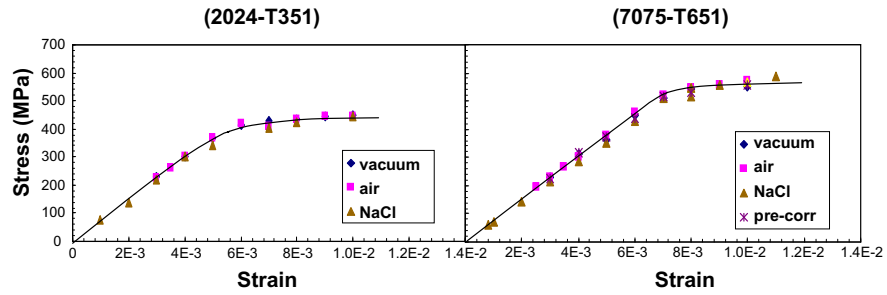


Fig. 4. Cyclic stress–strain curves of 2024-T351 and 7075-T651 aluminum alloys, LCF-tested in vacuum, air and 1% NaCl solution.

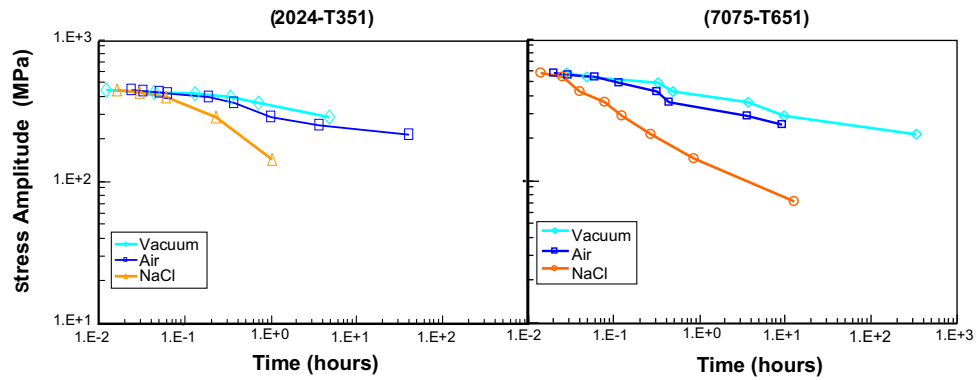


Fig. 5. Stress-time curves for 2024-T351 and 7075-T651 aluminum alloys, LCF-tested in vacuum, air and 1% NaCl solution.

vicinity of the crack initiation site, and shows initially faint and subsequently well-developed striations in the outside area, Fig. 6. The flat and featureless fractograph reflects un-resolvably small spacing of fatigue striation or very slow fatigue crack growth. In contrast, LCF testing in air produced bands of discernable striations near the crack initiation site, Fig. 6, indicating high crack growth rates. On the other hand, the LCF testing in 1% NaCl solution produced cleavage facets, separated by steps and exhibiting fan-like pattern, in the immediate vicinity of crack initiation site, Fig. 6. This feature evidences the environmentally-induced, possibly hydrogen, embrittlement. As the crack grows, the striations become the dominant fractographic features with increasing spacing, dimples are generated more and more, and eventually dimples replace the striations partially and entirely, approaching the final fracture, in those specimens tested in the three environments. An example is shown in Fig. 7. These fractographic features are observed to be unique for each environment and independent of the applied strain amplitude.

Similar observations were also made by the other investigators [15–17]. Meyn [15] found flat and featureless morphology in 2024-

T351 alloy specimen fatigued in vacuum and regular fatigue striations in the specimen fatigued in air. Bache et al. [16] reported the observation of striations in Inconel 718, fatigued in vacuum. Meyn [17] observed cleavages in Ti-8Al-1Mo-1V alloy fatigued in 3.5% NaCl solution. Girones et al. [25] reported the presence of brittle transgranular facets in duplex stainless steels, fatigued in a solution of 0.3 M H_3BO_3 , 0.075 M $Na_2B_4O_7 \cdot 10H_2O$ and 0.06 M $Na_2MoO_4 \cdot 2H_2O$, acidified with HCl to pH 2. They attributed it to hydrogen embrittlement. On the other hand, they observed fatigue striations in specimens tested in the solution of pH 8.4 and 6.

In the above discussion, an emphasis was placed on the features of fracture surface morphology in the immediate vicinity of crack initiation site in the 7075-T651 aluminum alloy specimens, subjected to LCF straining at an identical straining frequency 5 Hz in the three different environments. Therefore, the observed fracture surface morphological features are believed to reflect the distinct modes of threshold LCF crack growth, associated with the respective environments. Those modes are very slow threshold FCG with flat featureless morphology in vacuum, fast one with striation in air and much faster one with cleavage in 1% NaCl solution.

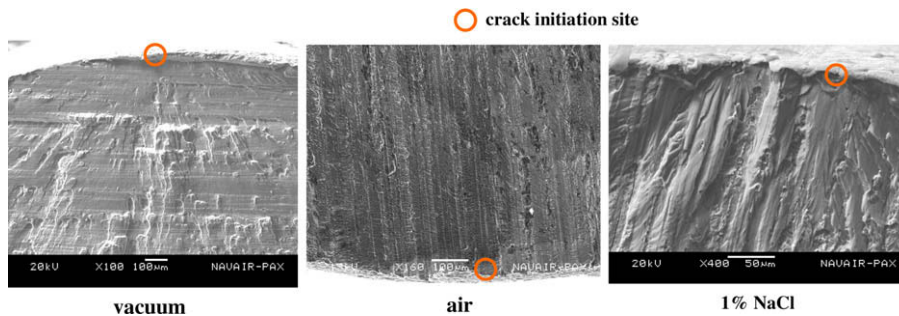


Fig. 6. SEM fractographs of 7075-T651 aluminum alloy specimens, LCF-tested in vacuum, air and 1% NaCl solution, showing the vicinity of crack initiation site.

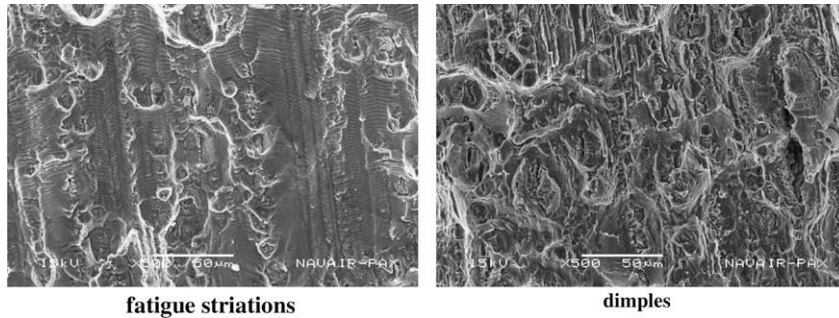


Fig. 7. SEM fractographs of 7075-T651 aluminum alloy specimen, LCF-tested in air, showing fatigue striations and dimples away from the vicinity of crack initiation site.

4. Summary and conclusion

1. LCF resistance is greatest in vacuum, less in air and least in 1% NaCl solution.
2. Intercept and slope of strain–life curve is least in vacuum, intermediate in air and greatest in 1% NaCl solution.
3. LCF lives of 2024-T351 and 7075-T651 aluminum alloys are similar in vacuum, air and 1% NaCl solution, respectively.
4. Pre-corrosion in 1% NaCl solution has little influence on the subsequent LCF life in air.
5. Cyclic stress–strain response is independent of environment but unique to the alloy.
6. Aggressive environment, 1% NaCl solution of pH 2, induces cleavage cracking in the immediate vicinity of crack initiation site, possibly due to hydrogen embrittlement in 7075-T651 aluminum alloy.
7. The mode of threshold LCF crack growth in 7075-T651 aluminum alloy is influenced by the environment: very slow FCG with flat featureless crack surface morphology in vacuum, fast one with striation in air, and much faster one with cleavage in 1% NaCl solution.

References

- [1] Duquette DJ. A mechanistic understanding of the effects of environment on fatigue crack initiation and propagation. In: Foroulis ZA, editor. Environment-sensitive fracture of engineering materials. Wattentale (PA): The Metallurgical Society of AIME; 1979. p. 521–37.
- [2] Shen H, Podlaseck SE, Kramer IR. Effect of vacuum on the fatigue life of aluminum. *Acta Metall* 1966;14(March):341–6.
- [3] Duquette DJ, Gell M. The effect of environment on the mechanism of stage I: fatigue fracture. *Metal Trans* 1971;2(May):1325–31.
- [4] Mendez J, Demulsant X. Influence of environment on low cycle fatigue damage in Ti-6Al-4V and Ti 6246 titanium alloys. *Mater Sci Eng A* 1996;219(1–2):202–11.
- [5] Mendez J. On the effects of temperature and environment on fatigue damage processes in Ti alloys and in stainless steel. *Mater Sci Eng* 1999;263(2): 187–92.
- [6] Jaske CE, Broek D, Slater JE, Anderson WE. Corrosion fatigue of structural steels in seawater and for offshore applications. *Corrosion fatigue technology*, ASTM STP 642. American Society for Testing and Materials; 1978. p. 19–47.
- [7] Henaff G, Odemer G, Tonneau-Morel A. Environmentally-assisted fatigue crack growth mechanisms in advanced materials for aerospace applications. *Int J Fatigue* 2007;29:1927–40.
- [8] Wei RP, Simmons GW. Recent progress in understanding environment-assisted fatigue crack growth. *Int J Fract* 1981;17(2):235–47.
- [9] Radon JC, Branco CM, Culver LE. Crack blunting and arrest in corrosion fatigue of mild steel. *Int J Fract* 1976;12:467–9.
- [10] Tu LKL, Seth BB. Threshold corrosion fatigue crack growth in steels. *J Test Eval* 1978;6(1):66–74.
- [11] Nordmark GE, Fricke WG. Fatigue crack arrest at low stress intensities in a corrosive environment. *J Test Eval* 1978;6(5):301–3.
- [12] Creager M, Paris PC. Elastic field equations for blunt cracks with reference to stress corrosion cracking. *Int J Fract Mech* 1967;3:247–52.
- [13] Vitek V. Plane strain intensity factors for branched cracks. *Int J Fract* 1977;13:481–501.
- [14] Vasudevan AK, Suresh S. Influence of corrosion deposits on near-threshold fatigue crack growth behavior in 2xxx and 7xxx series aluminum alloys. *Metal Trans A* 1982;13A:2271–8.
- [15] Meyn DA. The nature of fatigue crack propagation in air and vacuum for 2024 aluminum. *Trans Am Soc Metals* 1968;61(1):52–61.
- [16] Bache MR, Evans WJ, Hardy MC. The effect of environment and loading waveform on fatigue crack growth in Inconel 718. *Int J Fatigue* 1999;21: S69–77.
- [17] Meyn DA. An analysis of frequency and amplitude effects on corrosion fatigue crack propagation in Ti-8Al-1Mo-1V. *Metal Trans* 1971;2(3):853–65.
- [18] Driver JH, Gorlier C, Belrami C, Violan P, Amzallag C. Influence of temperature and environment on the fatigue mechanisms of single-crystal and polycrystal 316L. In: Solomon HD, Halford GR, Kaisand LR, Leis BN, editors. *Low cycle fatigue*, ASTM STP 942. American Society for Testing and Materials; 1988. p. 438–55.
- [19] Hoffman C, Eylon D, McEvily AJ. Influence of microstructure on elevated temperature fatigue resistance of a titanium alloy. In: Amzallag C, Leis BN, Rabbe P, editors. *Low cycle fatigue and life prediction*, ASTM STP 770. American Society for Testing and Materials; 1982. p. 5–22.
- [20] Wright PK. Oxidation-fatigue interactions in a single-crystal superalloy. In: Amzallag C, Leis BN, Rabbe P, editors. *Low cycle fatigue and life prediction*, ASTM STP 770. American Society for Testing and Materials, Berlin, pp. 558–575.
- [21] Coffin LF. A study of the effects of cyclic thermal stresses on a ductile metal. *Trans ASME* 1954;76:931–50.
- [22] Manson SS. Behavior of materials under conditions of thermal stress. NACA report 1170, 1954.
- [23] Ramberg W, Osgood WR. Description of stress–strain curves by three parameters. NACA technical note no. 902, July 1943.
- [24] Suresh S. *Fatigue of materials*. 2nd ed. Cambridge (UK): Cambridge University Press; 1998. p. 378.
- [25] Girones A, Mateo A, Llanes L, Anglada M, Deluccia J, Laird C. Evaluation of fatigue damage for duplex stainless steels in aggressive environments by means of an electrochemical fatigue sensor (EFS). *Int J Fatigue* 2003;25: 1189–94.